Particle Accelerators
1983 Vol. 13 pp. 231–247
0031-2460/83/1303/0231$06.50/0

SPACE-CHARGE LIMITS IN HEAVY-ION RFQ LINACS

P. JUNIOR

Institut für Angewandte Physik der J. W. Goethe-Universität Frankfurt/Main, Robert-Mayer-Str. 2-4, D-6000 Frankfurt/Main, Germany

(*Received October 5, 1982; in final form March 14, 1983*)

Voltage, aperture, frequency and input energy determine the maximum beam current in the RFQ linac. Theoretical calculations require considerable computational efforts. In this paper we derive analytical approximation formulas for the relevant quantities in RFQ linac design, namely, beam current, phase advances, acceptances, and partition of temperatures.

INTRODUCTION

In the Institute für Angewandte Physik of the University of Frankfurt, a RFQ structure is being developed for heavy-ion fusion demands, which consists of electrode rods, manufactured on a lathe.[1] The profile is trapezoidal, the rods are stemmed periodically and because of necessary low-frequency operation, the resonators are excited in zero mode.[2,3] A theoretical discussion of sparking limits with respect to voltage, frequency, and aperture took place at GSI,[4] where we presented computations with the remarkable result that beam current is approximately proportional to voltage independent of frequency (6.78, 9.04, 13.56 MHz) and aperture (0.6 and 1.5 cm). It will be shown within the framework of an analytical theory that this behavior can be explained.

1. EQUATIONS OF MOTION

Instead of the trapezoidal rods proposed in our designs,[1–4] we will use the ideal profile[5] here, because we need closed relations for the RFQ parameters. Instead of the usual expressions, which use modified Bessel funtions[5,6] we represent the potential with hyperbolic functions as

$$\Phi(x, y, z, t) = \frac{V}{2} \sin(\omega t - \phi_s)\left[C_0 \frac{x^2 - y^2}{R_1^2} + \frac{A_1}{2} \cos kz(\cosh kx + \cosh ky)\right]. \tag{1}$$

This representation proves suitable for several reasons. First, microcomputers are usually equipped with the exponential function. Furthermore, treatment of electrodes with higher-harmonic spatial modulation corresponds to terms as simple as $A_N/2 \cos NKz\,(\cosh NKx \pm \cosh NKy)$ in the expansions. The corresponding electrode scheme is illustrated in Fig. 1. The coefficients A_1 and C_0 depend on

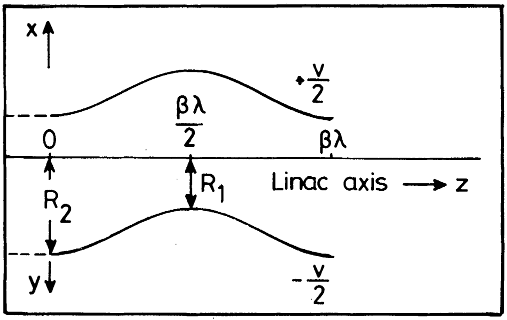

FIGURE 1 Scheme of ideal electrode intersections at $y = 0$ resp. $x = 0$, the ideal profile being spatially represented by

$$C_0 \frac{x^2 - y^2}{R_1{}^2} + \frac{1}{2} A_1 \cos \frac{2\pi}{\beta\lambda} z \left(\mathrm{ch} \frac{2\pi}{\beta\lambda} x + \mathrm{ch} \frac{2\pi}{\beta\lambda} y \right) = \pm 1,$$

where $\pm$ corresponds to quadrupole electrode pairs resp.

geometrical dimensions according to

$$\begin{aligned} A_1 &= 2 \frac{R_2{}^2 - R_1{}^2}{R_1{}^2(1 + \cosh kR_2) + R_2{}^2(1 + \cosh kR_1)} \\ C_0 &= R_1{}^2 \frac{2 + \cosh kR_1 + \cosh kR_2}{R_1{}^2(1 + \cosh kR_2) + R_2{}^2(1 + \cosh kR_1)} \end{aligned} \tag{2}$$

and are linked to each other by the relation

$$C_0 + \frac{A_1}{2}(1 + \cosh kR_1) = 1, \tag{3}$$

where $k = 2\pi/\beta\lambda$ is the longitudinal wave number. From Eq. (1), linear equations of motion can be deduced, i.e. for the transverse motion of synchronous particles

$$\begin{aligned} \frac{d^2x}{d\tau^2} + \left(a + 2q \cos 2\tau - \frac{\gamma F_x}{a_x a_y a_u} \right) x = 0 \\ \frac{d^2y}{d\tau^2} + \left(a - 2q \cos 2\tau - \frac{\gamma F_y}{a_x a_y a_u} \right) y = 0 \end{aligned} \tag{4}$$

and for the longitudinal motion of particles on the axis

$$\frac{d^2u}{d\tau^2} - \left(2a + \frac{\gamma F_u}{a_x a_y a_u} \right) u = 0. \tag{5}$$

With the abbreviations chosen, we follow the notation[7] for Mathieu's equation, where the dimensionless time variable

$$\tau = \frac{1}{2}(\omega t - \phi_s) \tag{6}$$

corresponds to the period π of the linac. The Mathieu equation parameters are given by

$$a = -\frac{eVA_1 \sin \phi_s}{2mv^2} \tag{7}$$

and

$$q = \frac{2eVC_0}{m\omega^2 R_1{}^2}. \tag{8}$$

Space charge is expressed by

$$\gamma = \frac{3eQ}{m\omega^2 \pi \epsilon_0}. \tag{9}$$

Here e/m is the specific charge of the ion, V the voltage between electrodes, ϕ_s the synchronous phase, v the synchronous velocity, $f = \omega/2\pi$ the frequency of the linac and ϵ_0 the dielectric constant.

For space charge the K-V[8] setting is extended to 3 dimensions. The beam bunch is understood as an ellipsoid with semiaxes a_x, a_y, a_u uniformly filled by the total charge Q. Thus a mean beam current

$$I = fQ \tag{10}$$

should be inserted in Eqs. (4) and (5).

In the case of a continuous beam in the longitudinal direction, uniform charge density ρ_{DC} in the corresponding elliptical cylinder with length a_u

$$\rho_{DC} = \frac{Q}{\pi a_x a_y a_u}$$

gives the direct beam current

$$I_{DC} = \frac{3v}{4a_u} Q, \tag{11}$$

which should then be inserted in Eq. (4).

Closed formulas do not exist in the general cases for the formfactors F_x, F_y, F_u appearing as functions of the three beam envelopes at any situation τ. A smooth-approximation formalism requires simplifications, however, which we do by using the expressions

$$F_x = \frac{a_y}{a_x + a_y}(1 - F_u)$$

$$F_y = \frac{a_x}{a_x + a_y}(1 - F_u)$$

$$F_u = \frac{\bar{a}_t}{3a_u} \qquad \text{with } \bar{a}_t = \sqrt{a_x a_y}. \tag{12}$$

F_u is given according to,[11,12] where the case of the rotational ellipsoid ($a_x = a_y = a_t$) is discussed. F_x and F_y generally differ from each other, however, corresponding to different transverse semiaxes of the ellipsoid; they are derived from the K-V expressions for a longitudinally infinite beam.[8] The finite bunch length is taken into account by the corrections

$$\frac{a_x F_u}{a_x + a_y} \quad \text{and} \quad \frac{a_y F_u}{a_x + a_y}.$$

Figure 2 shows us that the approximations (12) are feasible in the range

$$0 \leqq \sqrt{a_x a_y} \leqq a_u. \tag{13}$$

With the approximations of Eq. (12), envelope equations can be derived from Eqs. (4) and (5). Then

$$\begin{aligned}
&\frac{d^2 a_x}{d\tau^2} + (a + 2q\cos 2\tau)a_x - \frac{\gamma\left(1 - \dfrac{\bar{a}_t}{3a_u}\right)}{a_u(a_x + a_y)} - \frac{\epsilon_t^2}{a_x^3} = 0\\
&\frac{d^2 a_y}{d\tau^2} + (a - 2q\cos 2\tau)a_y - \frac{\gamma\left(1 - \dfrac{\bar{a}_t}{3a_u}\right)}{a_u(a_x + a_y)} - \frac{\epsilon_t^2}{a_y^3} = 0
\end{aligned} \tag{14}$$

$$\frac{d^2 a_u}{d\tau^2} - 2aa_u - \gamma\frac{1}{3\bar{a}_t a_u} - \frac{\epsilon_1^2}{a_u^3} = 0. \tag{15}$$

Here ϵ_t and ϵ_1 are the transverse and longitudinal emittances, i.e. ellipse areas divided by π in the phase space x, $dx/d\tau$, y, $dy/d\tau$, u, $du/d\tau$, where the dimensionless variable τ is implied. The coventional emittance in terms of coordinate and velocity is obtained by multiplying by $\omega/2$. The transverse emittances are taken to be identical.

A beam is considered as matched, when the envelope functions $a_x(\tau)$, $a_y(\tau)$, $a_u(\tau)$ have the linac period. Any linac section is matched to it's predecessor when all three phase advances, not depressed by space charge, are fixed, first of all along the buncher sections. With fixed apertures along the linac the envelopes and the acceptance ellipses reproduce at the end of each section. This means in the case of the longitudinal motion of Eq. (5)

$$\frac{A_1 \sin\phi_s}{v^2} = \text{const.} \tag{16}$$

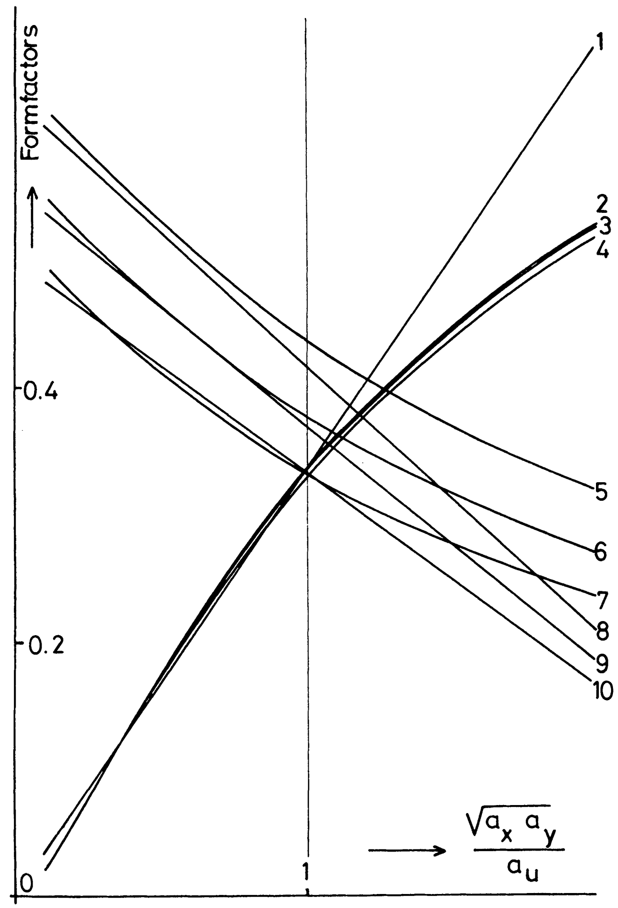

FIGURE 2 Formfactor approximation

1. F_u approximation Eq. (12)
2. F_u exact $a_x/a_y = 1.0$
3. F_u exact $a_x/a_y = 0.8$
4. F_u exact $a_x/a_y = 0.6$
5. F_x exact $a_x/a_y = 0.6$
6. F_x exact $a_x/a_y = 0.8$
7. F_x exact $a_x/a_y = 1.0$
8. F_x approximations $a_x/a_y = 0.6$
9. F_x approximations $a_x/a_y = 0.8$
10. F_x approximations $a_x/a_y = 1.0$

For the determination of the acceptance ellipses needed, we take as maximum transverse semiaxes the minimum aperture radius R_1 (see Fig. 1). For the longitudinal case we use the expression

$$a_{u,\max} = \frac{v}{\pi f}\sqrt{1 - \phi_s \operatorname{ctg} \phi_s}, \tag{17}$$

which can easily be derived by approximating the separatrix by an ellipse and taking it's angular semiaxis.[10] The applicability of Eq. (17) is demonstrated in Fig. 3.

When the longitudinal aperture of Eq. (17) is kept constant along the buncher, velocities and synchronous phases in subsequent $\beta\lambda$ sections are determined by

$$v_{\text{out}} = v_{\text{in}} \sqrt{\frac{1 - \phi_{\text{in}} \operatorname{ctg} \phi_{\text{in}}}{1 - \phi_{\text{out}} \operatorname{ctg} \phi_{\text{out}}}}. \tag{17a}$$

As a consequence, the velocity gain of the synchronous particle after passing *a* $\beta\lambda$ section

$$v_{\text{out}} = \sqrt{v_{\text{in}}^2 + \frac{e\pi}{m} VA_1 \cos \phi_{\text{in}}}$$

determines the synchronous phase ϕ_{out} of the subsequent section. This rule is being followed throughout in our designs. Equation (17) is given preference here to the better-known implicit formula for the total stable phase range $\Delta\phi$

$$\tan \phi_s(1 - \cos \Delta\phi) + \sin \Delta\phi - \Delta\phi = 0,$$

because Eq. (17) implies an explicit expression for the longitudinal aperture, although the assumption seems slightly pessimistic. In general, Eqs. (14) and (15) form a coupled system of nonlinear differential equations with complicated solutions. Approximate results can be derived, however, as will be shown in the following sections.

2. SMOOTH-APPROXIMATION THEORY

A. Smooth Longitudinal Envelope

In this section the smooth-approximation formalism is applied first for the simpler case of the longitudinal envelope. We substitute in Eqs. (14) and (15) by

$$\begin{aligned} a_x &= \bar{a}_t(1 + \delta_x(\tau)) \\ a_y &= \bar{a}_t(1 + \delta_y(\tau)), \end{aligned} \tag{18}$$

where the deviations $\bar{a}_t\delta_x(\tau)$ and $\bar{a}_t\delta_y(\tau)$ are considered small compared to the constant mean transverse aperture $\bar{a}_t$, then all coefficients in Eq. (15) are constant, admitting a constant solution

$$\bar{a}_u = \sqrt{-\frac{\gamma}{12a\bar{a}_t} + \sqrt{\left(\frac{\gamma}{12a\bar{a}_t}\right)^2 - \frac{\epsilon_1{}^2}{2a}}}. \tag{19}$$

Apart from the assumed smooth behaviour of transverse envelopes Eq. (19) is an exact solution of Eq. (15) and in fact corresponds, with linac period π, to the longitudinally matched beam. When we identify the constant envelope radius of Eq. (19) with the aperture of Eq. (17), the emittance becomes the acceptance and Eq. (19) offers a relation between aperture and acceptance.

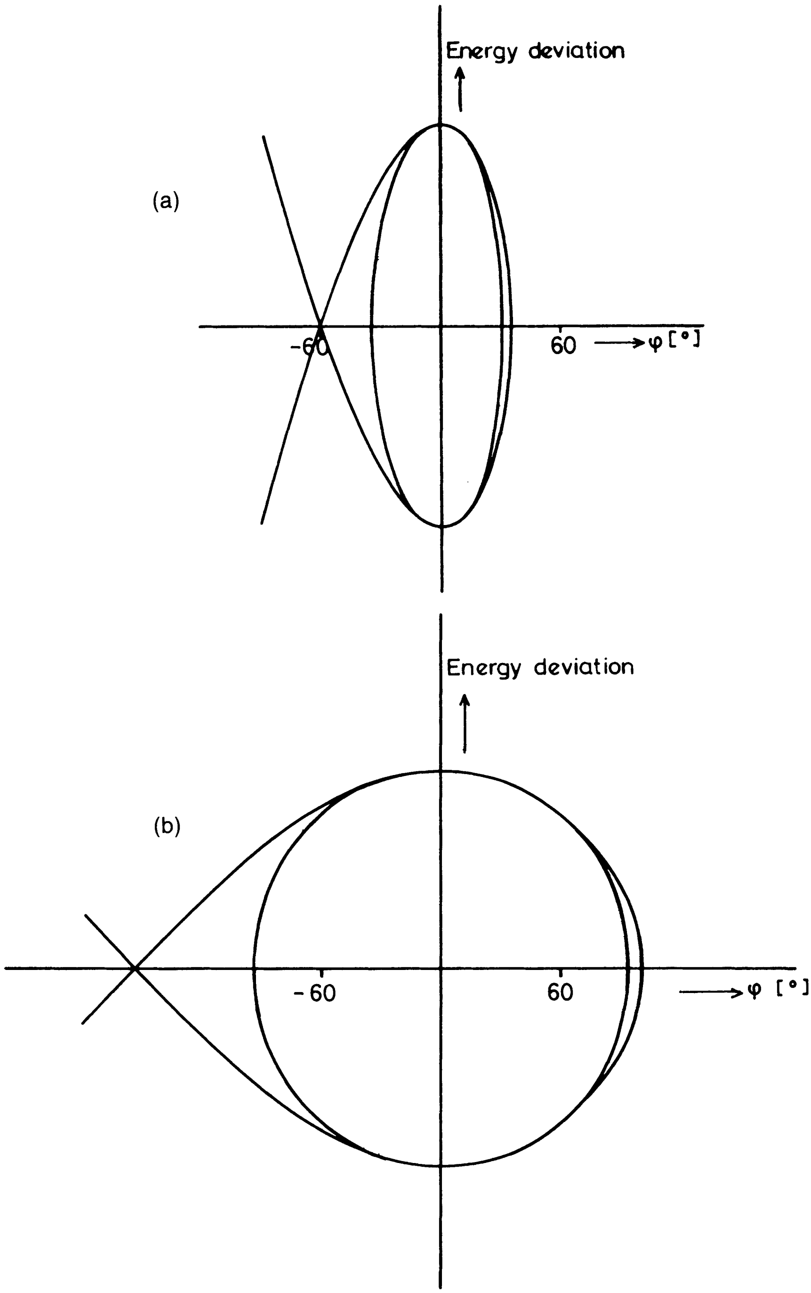

FIGURE 3 Ellipse approximation of (a) separatrix for $\phi_s = 30°$ (b) separatrix for $\phi_s = 77°$.

Then for any matched beam, there exists a further general relation between emittance and mean envelope radius[9]

$$\frac{\sigma}{\pi} = \frac{\epsilon}{\bar{a}^2}, \tag{20}$$

where σ is the phase advance per period. With the index 0 corresponding to $Q = 0$, the following relations can easily be derived from Eq. (19) supposing identical aperture radius $\bar{a}_u$ with and without space charge, and consequently resulting in different acceptance areas

$$\begin{aligned} \epsilon_{01}^2 &= -2a\bar{a}_u{}^4 \\ \epsilon_1{}^2 &= \epsilon_{01}^2 - \frac{\gamma\bar{a}_u{}^2}{3\bar{a}_t} \end{aligned} \tag{21}$$

$$\begin{aligned} \frac{\sigma_{01}^2}{\pi^2} &= -2a \\ \frac{\sigma_1{}^2}{\pi^2} &= \frac{\sigma_{01}^2}{\pi^2} - \frac{\gamma}{3\bar{a}_t\bar{a}_u{}^2} \end{aligned} \tag{22}$$

Tune- and acceptance depressions are then identical

$$\frac{\sigma_1}{\sigma_{01}} = \frac{\epsilon_1}{\epsilon_{01}}. \tag{23}$$

B. Smooth Transverse Envelopes

Inserting Eqs. (18) and (19) in Eq. (14), the following linear equations are derived, assuming small derivations $\delta_x(\tau)$, $\delta_y(\tau) \ll 1$ and using Eq. (20) for the transverse phase advance

$$\begin{aligned} &\frac{d^2\delta_x}{d\tau^2} + \left[a + 2q\cos 2\tau + \frac{\gamma}{4\bar{a}_u\bar{a}_t{}^2}\left(1 - \frac{\bar{a}_t}{3\bar{a}_u}\right) + 3\frac{\sigma_t{}^2}{\pi^2}\right]\delta_x + \frac{\gamma}{4\bar{a}_u\bar{a}_t{}^2}\left(1 - \frac{\bar{a}_t}{3\bar{a}_u}\right)\delta_y \\ &\quad = -a - 2q\cos 2\tau + \frac{\gamma}{2\bar{a}_u\bar{a}_t{}^2}\left(1 - \frac{\bar{a}_t}{3\bar{a}_u}\right) + \frac{\sigma_t{}^2}{\pi^2}. \end{aligned} \tag{24}$$

From Eq. (14), we see with $a_x(\tau + \pi/2) = a_y(\tau)$ that

$$\delta_x\left(\tau + \frac{\pi}{2}\right) = \delta_y(\tau). \tag{25}$$

Again the matched beam requires π-periodicity of the solution and this can only be realized by solving the inhomogeneous equations, the homogeneous corresponding to a smaller frequency. Thus the matched solutions $\delta_x(\tau)$, $\delta_y(\tau)$ can generally be written as Fourier series

$$\delta_x = a_2 \cos 2\tau + a_4 \cos 4\tau + \cdots$$
$$\delta_y = b_2 \cos 2\tau + b_4 \cos 4\tau + \cdots, \tag{26}$$

where $b_{4N-2} = -a_{4N-2}$, $b_{4N} = a_{4N}$ for $N = 1, 2, 3, \ldots$ are consequences of Eq. (25). Inserting Eq. (26) in Eq. (24) and equating coefficients to zero the constant term yields

$$qa_2 = \frac{\sigma_t^2}{\pi^2} + \gamma \frac{1 - \dfrac{\bar{a}_t}{3\bar{a}_u}}{2\bar{a}_t^2\bar{a}_u} - a, \tag{27}$$

while the cos 2τ term appears with

$$a_4 q + 2q + a_2\left(-4 + a + \frac{3\sigma_t^2}{\pi^2}\right) = 0 \tag{28}$$

From Eqs. (27) and (28) with small phase advance $\sigma_t^2 \ll 4/3\pi^2$ and small defocusing term $|a| \ll 4$, simple expressions for the depressed and undepressed phase advances, together with the first-order Fourier coefficient can be derived

$$\frac{\sigma_t^2}{\pi^2} = \frac{\sigma_{0t}^2}{\pi^2} - \gamma \frac{1 - \dfrac{\bar{a}_t}{3\bar{a}_u}}{2\bar{a}_t\bar{a}_u} \tag{29}$$

$$\frac{\sigma_{0t}^2}{\pi^2} = \frac{q^2}{2} + \mathrm{a} \tag{30}$$

$$a_2 = \frac{q}{2}. \tag{31}$$

The validity of Eq. (30) is illustrated in the stability chart of Mathieu's equation in Fig. 4. Obviously, the smooth approximation is in good agreement with exact calculation as long as $\sigma_0 < 30°$. Beyond that the deviations increase.

When we identify the transverse beam emittance with the acceptance related to the smallest RFQ aperture R_1, an expression

$$R_1 \doteq \bar{a}_t\left(1 + \frac{q}{2}\right) \tag{32}$$

can be derived from Eqs. (18), (26) and (31).

Assuming small phase advances leading to Eqs. (29) and (31), all Fourier coefficients of higher order can easily be estimated as small compared to a_2. Thus the smooth approximation leaves us with the remarkable result that according to Eqs. (26), (31) and (32), the matched beam flutters independent of space charge. In other words, reflecting Eqs. (18) and (19) we can say that the matched beam behaves like an incompressible liquid, the beam volume remaining constant throughout regardless of space charge.

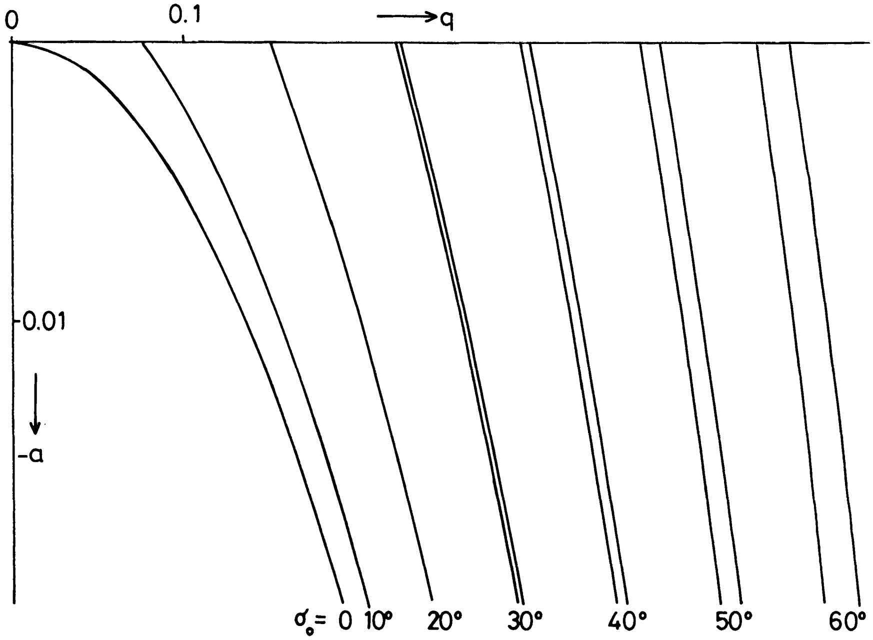

FIGURE 4 Iso-σ-curves of Mathieu's equation: Left curve exact calculation, right curve smooth approximation resp., ranges of a and q corresponding to realistic RFQ dimensions.

C. Currents

With Eqs. (9), (10) and (22) the beam current is either longitudinally limited by the condition $\sigma_1 = 0$, giving

$$I_1^{\max} = \frac{\epsilon_0 m\omega^3 \bar{a}_t \bar{a}_u{}^2 \sigma_{01}^2}{2e\pi^2} \tag{33}$$

or this happens with transverse phase advance $\sigma_t = 0$, resulting in

$$I_t^{\max} = \frac{\epsilon_0 m\omega^3 \bar{a}_t \bar{a}_u{}^3 \sigma_{0t}^2}{e\pi^2(3\bar{a}_u - \bar{a}_t)} \tag{34}$$

where Eqs. (9), (10) and (29) have been employed. When we replace the longitudinal phase advance (22) in Eq. (33) by the transverse one (30) using Eqs. (3), (7) and (8), the dependence of the currents (33) and (34) on the transverse phase advance is illustrated in Fig. 5. Before utilizing these relations, attention should be drawn to the particular case of the *dc* beam. Supposing it longitudinally infinite, which corresponds to the formfactors (12) with $F_u = 0$ and using Eq. (11) instead of Eq. (10), we are led to the expression

$$I_t^{dc} = \frac{\epsilon_0 m\omega^3 \bar{a}_t{}^2 V}{4ef} \frac{\sigma_{0t}^2 - \sigma_t{}^2}{\pi^2} \tag{35}$$

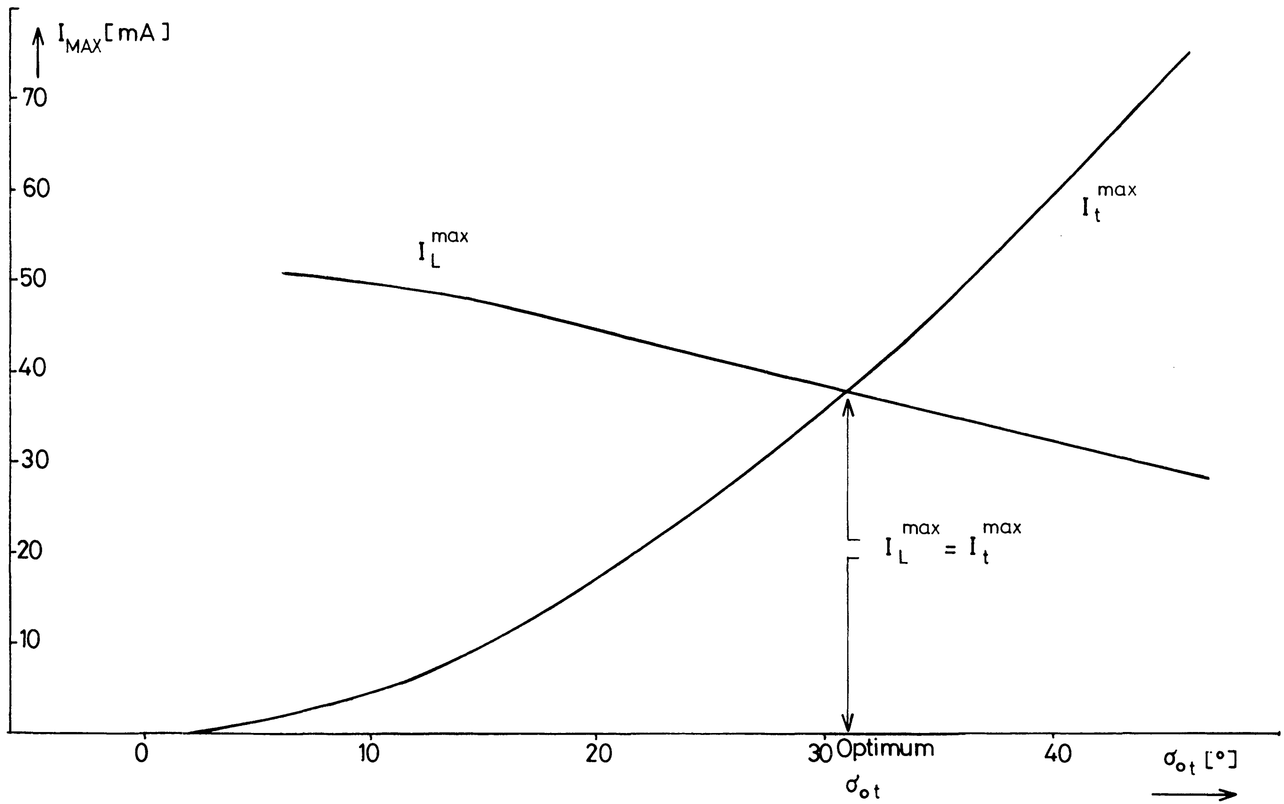

FIGURE 5 Maximum longitudinal and transverse currents, optimum transverse phase advance

Data: Cs^{1+}_{133} $v = 2.24 \cdot 10^6$ m/s $V = 150$ kV $R_1 = 0.6$ cm $f = 13.56$ MHz $\phi_s = 30^0$

Then with the relations $\bar{a}_t = \sqrt{v\eta/f\sigma_0}$ (where η is the acceptance in the $x - dx/dz$ plane), $s = v/f$ (s is the length of a quadrupole period) and the abbreviation

$$I_0 = \frac{4\pi\epsilon_0 mc^3}{e}, \tag{36}$$

Equation (35) fully agrees with Reiser's formula given in.[14]

While conventional linac parameters usually make it impossible to satisfy the condition[†]

$$\frac{\sigma_{01}^2}{\sigma_{0t}^2} = \frac{2\bar{a}_t}{3\bar{a}_u - \bar{a}_t}, \tag{37}$$

that is, attaining both limits (33) and (34) simultaneously and thus admitting the maximum beam current in general, the RFQ allows this opportunity, at least in heavy-ion applications. Figure 5 illustrates an example.

When we inspect Eq. (37), it seems reasonable that the spherical bunch $\bar{a}_t = \bar{a}_u$ corresponds to equal phase advances. Inserting Eqs. (21), (30) and (32) in Eq. (37) a condition between the RFQ parameters abbreviated by Eqs. (7) and (8) follows:

$$\frac{R_1 9^2}{6\bar{a}_u\left(1 + \frac{q}{2}\right)} = -a \tag{38}$$

a second relation comes from Eqs. (3), (7) and (8)

$$\frac{\alpha^2}{2} q = \chi + \kappa a, \tag{39}$$

where we have abbreviated

$$\alpha = \frac{\omega}{v} R_1, \qquad \chi = \frac{eV}{mv^2}, \qquad \kappa = \frac{1 + \cosh\alpha}{\sin\phi_s}. \tag{40}$$

Eliminating a and q from Eqs. (38) and (39), the optimized RFQ parameter is given by

$$q = P\left[\sqrt{1 + \frac{O}{P^2}} - 1\right], \tag{41}$$

with

$$O = \frac{4\chi}{\frac{2R_1\kappa}{3\bar{a}_u} + \alpha^2} \tag{42}$$

[†] The example chosen in [13] demonstrates this inconvenience.

and

$$P = \frac{\alpha^2 - \chi}{\dfrac{2R_1\kappa}{3\bar{a}_u} + \alpha^2}$$

Equation (33) together with Eqs. (38), (17), (36) and (40) now gives the optimized maximum beam current (see Fig. 5)

$$I_1^{\max} = I_t^{\max} = I_0 \frac{\beta^3}{\pi} \frac{\alpha}{1 + \cosh\alpha} (\sin\phi_s - \phi_s \cos\phi_s) \frac{\chi - \dfrac{\alpha^2}{2} q}{1 + \dfrac{q}{2}}, \tag{43}$$

an expression, which involves only ϕ_{s0}, ϕ_s, v_0, v, ω, V, R_1.

When designing a RFQ with respect to maximum beam current, the optimal transverse phase advance informs us on the stability of the beam transport and can easily be calculated from

$$\frac{\sigma_{0t}^2}{\pi^2} = \frac{\chi - \dfrac{\alpha^2}{2} q}{1 + \mathrm{ch}\alpha} \sin\phi_s \left[\frac{6}{\alpha} \sqrt{1 - \phi_s \,\mathrm{ctg}\,\phi_s} \left(1 + \frac{q}{2}\right) - 1 \right]. \tag{44}$$

Both expressions are illustrated in Figs. 6 and 7.

Contributions of terms involved in Eqs. (43) and (44) are listed in Table I, representing typical RFQ design parameters, i.e., Cs_{133}^{1+}-ion, velocity $2.24 \cdot 10^6$ m/s corresponding to an ion energy of 3.48 MeV at the end of the gentle buncher with $\phi_s = 30°$. The input velocity with Eq. (17a) of $0.82 \cdot 10^6$ m/s corresponds to an injection energy of 470 keV, where bunching starts with $\phi_s = 77°$.

This conversion of velocities is generally necessary for the correct evaluation of the implicit quantity α, as the electrode radius R_1 occuring usually does not initially agree with the beam radius. As a consequence of the transverse phase advance (30) being kept constant, the buncher starts with a rather large aperture, then adiabatically proceeds towards the final dimensions, where R_1 and ϕ_s remain fixed.

The voltages chosen correspond to Kilpatrick's[16] peak surface fields as discussed in Ref. 4. Table I also gives the weak dependence of terms $1 + \cosh\alpha$ and $1 + q/2$ on the parameters. The Mathieu parameter q, which according to Eqs. (26) and (31) plays the role of the "flutter factor", is small compared with 1. But this is postulated by the smooth approximation anyway.

The term α of the order R_1/a_u using Eq. (17) is smaller than 1, but not much smaller. As a consequence $\alpha^2 q/2$ can generally not be neglected compared with χ but because q increases monotonically with voltage, the almost constant slopes of the beam current (43) in Fig. 6 are thus explained. When we check the capability of the formfactor approximations (12), Eq. (17) leads us to longitudinal apertures $a_u =$ 1.59 cm at 13.56 MHz or 2.38 cm at 9.04 MHz. Then, using Eq. (32), the aperture ratios at the chosen transverse apertures $R_1 = 0.6$ cm and 1.5 cm do satisfy the condition

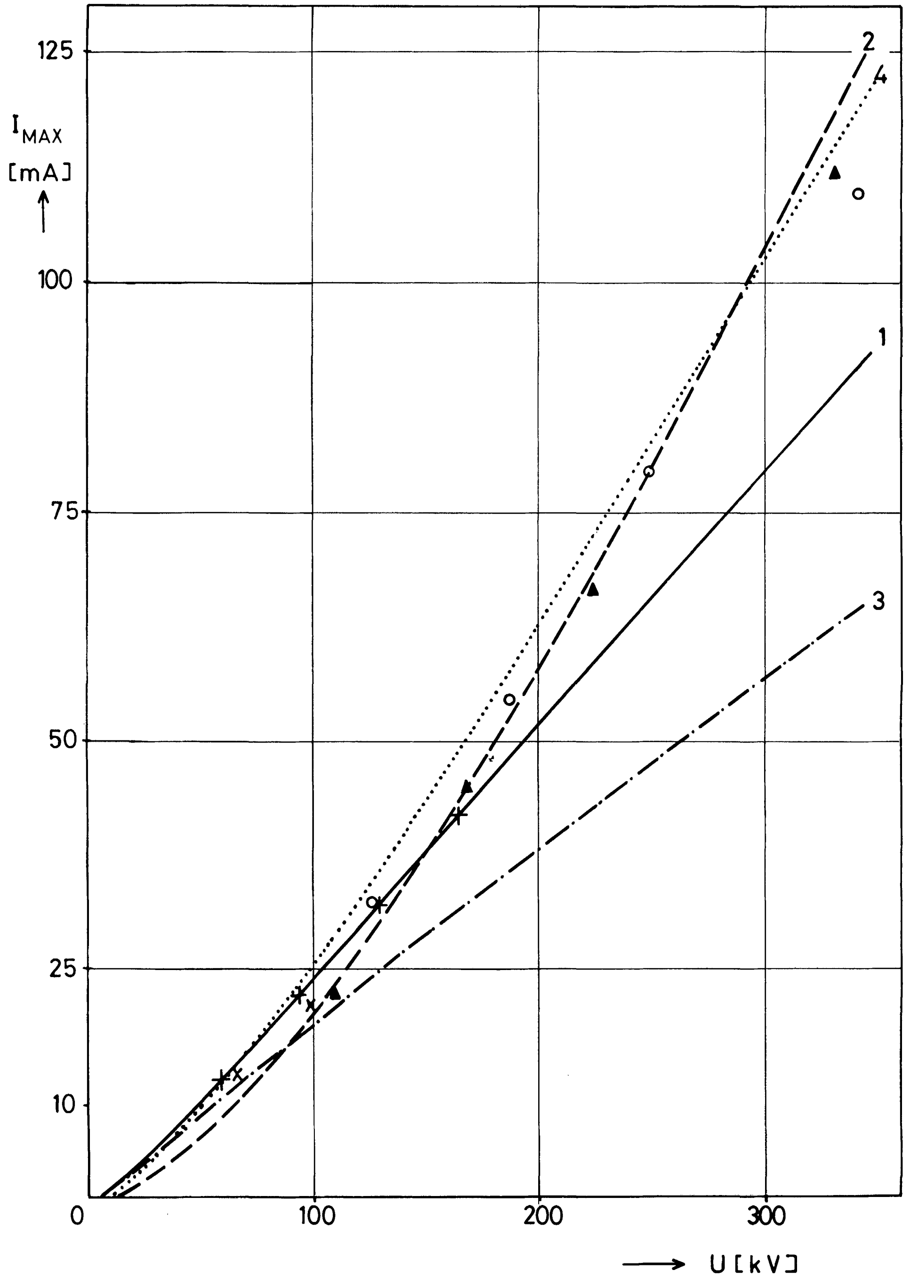

FIGURE 6 Maximum beam current $I_{\max} = I_t^{\max} = I_1^{\max}$

Marked points + ▲ × 0 result from exact calculations

Curve 1 —— 13.56 MHz, $R_1 = 0.6$ cm, points +

Curve 2 ----- 13.56 MHz, $R_1 = 1.5$ cm, points ▲

Curve 3 -·-·- 9.04 MHz, $R_1 = 0.6$ cm, points x

Curve 4 ····· 9.04 MHz, $R_1 = 1.5$ cm, point 0

Further data: $v = 2.24 \cdot 10^6$ m/s, ion Cs^{1+}_{133}

synchronous phase at buncher input $\phi_s = 77°$

synchronous phase at buncher output $\phi_s = 30°$.

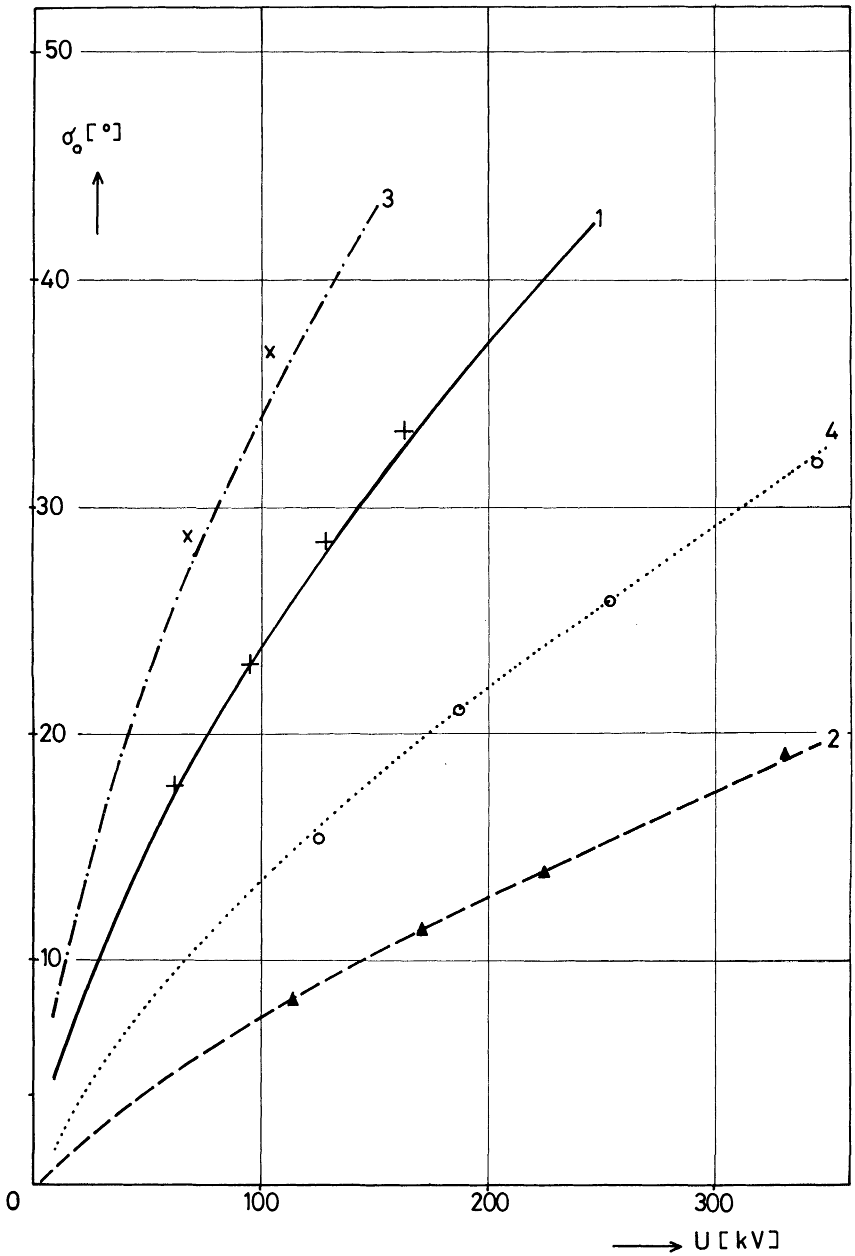

FIGURE 7 Optimum transverse phase advances for marked points and curves of Fig. 6.

TABLE I

Multiple of Kilpatrick's limit	1	2	1	2	1	2	1	2
Curve of fig. 6	1	1	2	2	3	3	4	4
U [kV]	62	124	113	225	69	138	125	250
α	0.23	0.23	0.57	0.57	0.15	0.15	0.38	0.38
$\chi \cdot 10^{-2}$	0.89	1.78	1.61	3.21	0.99	1.98	1.77	3.54
q	0.15	0.23	0.08	0.13	0.22	0.34	0.14	0.22
$\frac{\alpha^2 q}{2} \cdot 10^{-2}$	0.4	0.6	1.3	2.1	0.25	0.4	1.0	1.6

(13). In addition, Eqs. (25) and (32) give an estimate of the transverse envelope ratio

$$\frac{a_x}{a_y} = \frac{1 - \frac{q}{2}}{1 + \frac{q}{2}} \approx 1 - q,$$

again demonstrating the applicability of Eq. (12), which is illustrated in Fig. 2 for various ratios. Deviations at marked check points in Figs. 6 and 7 demonstrate violations of smooth-approximation assumptions, mainly resulting from formfactor errors (12) or too-large transverse phase advances, corresponding to somewhat unrealistic voltages.

D. *Precautions*

According to present opinion, any tune depression σ/σ_0 should not be chosen less than 0.4 in order to avoid emittance growth. Thus the corresponding current should not exceed 0.84 $I_{\max}$ because of Eqs. (9), (10), (20) and (29).

A further application of the smooth-approximation formalism lies in the easy determination of temperature conditions. In[15,17,18] the importance of equipartitioning is claimed. The corresponding temperature law

$$T \sim \epsilon\sigma$$

gives, with Eqs. (20) and (37), the ratio of longitudinal to transverse temperature at identical tune depressions for both motions

$$\frac{T_l}{T_t} = \frac{2\bar{a}_u^{\,2}}{3\bar{a}_u\bar{a}_t - \bar{a}_t^{\,2}}.$$

This is solely dependent on the aperture ratio. Obviously equipartition is optimal, when apertures and frequencies are properly chosen. The particular case of identical apertures then corresponds to identical temperatures.

CONCLUSIONS

For the evaluation of parameters involved in formulas for the optimum beam current (43) and the corresponding transverse phase advance (44), the equations required are I_0 from Eq. (36), $\beta = v/c$ from Eq. (17a), q from Eq. (41) together with Eq. (42); the parameters α, κ, χ are defined by Eq. (40), a_u by Eq. (17).

The following data are needed; rf voltage V, synchronous phase ϕ_{in} and ϕ_{out} at buncher in- and output resp., frequency $\omega/2\pi$, final aperture R_1, input velocity v_{in} and charge-to-mass ratio e/m of ion to be accelerated.

Equation (43) gives a fast guide for the determination of the beam current that can be expected in a properly designed RFQ linac. Furthermore eq. (44) informs us on the stability of the system. For these calculations, a microcomputer or slide rule suffices.

REFERENCES

1. P. Junior et al., 1981 Linear Accelerator Conference, Santa Fe, LA-9234-C, 1982 p. 81.
2. H. Klein et al., *ibid.* p. 96.
3. H. Klein et al., GSI Fusion Symp. 1982, GSI-Report 82–8, 1982 p. 150.
4. P. Junior et al., GSI Fusion Symp. 1982, GSI-Report 82–8, 1982 p. 248.
5. K. R. Crandall et al., 1979 Linear Accelerator Conference, Montauk, BNL-51134, 1979, p. 205.
6. I. M. Kapchinskii and N. V. Lazarev, *IEEE Trans. Nucl. Sci.*, **NS-26,** 3462 (1979).
7. N. W. McLachlan, *Theory and Applications of Mathieu Functions* (Clarendon Press, Oxford 1947).
8. I. M. Kapchinskii and V. V. Vladimirskii, Proceedings International Conference on High Energy Accelerators, CERN, Geneva, 1959, p. 274.
9. E. D. Courant and H. S. Snyder, *Ann. Phys.*, **3** (1958).
10. P. Junior, Inst. f. Angew. Physik, Univ. Frankfurt/M., Int. Rep. 80–10, 1980, unpublished.
11. T. P. Wangler, Space Charge Limits in Linear Accelerators, Los Alamos Rep. LA 8388, 1980.
12. R. L. Gluckstern, "Space Charge Effects" in *Linear Accelerators* by P. H. Lapostolle and A. I. Septier (North Holland Publishing Company, Amsterdam 1970).
13. M. Reiser, *J. Appl. Phys.*, **52,** 2 (1981).
14. M. Reiser, *Particle Accelerators,* **8,** 167 (1978).
15. R. A. Jameson, 1981 Linear Accelerator Conference Santa Fe, LA-9234-C, 1982, p. 125.
16. W. D. Kilpatrick, UCRL-2321, Univ. of California, Berkeley, 1953.
17. I. Hofmann, *IEEE Trans. Nucl. Sci.*, **NS-28,** 2399 (1981).
18. I. Hofmann and I. Bozsik, 1981 Linear Accelerator Conference, Santa Fe, LA-9234-C, 1982, p. 116.